

## REVIEW ARTICLE

# Induction coil sensors—a review

Slawomir Tumanski

Institute of Electrical Theory & Measurement, ul Koszykowa 75, 00-661 Warsaw, Poland

E-mail: [tusla@iem.pw.edu.pl](mailto:tusla@iem.pw.edu.pl)

Received 17 August 2006, in final form 7 November 2006

Published 19 January 2007

Online at [stacks.iop.org/MST/18/R31](http://stacks.iop.org/MST/18/R31)

### Abstract

This review describes induction coil sensors, which are also known as search coils, pickup coils or magnetic loop sensors. The design methods for coils with air and ferromagnetic cores are compared and summarized. The frequency properties of coil sensors are analysed and various methods for output signal processing are presented. Special kinds of induction sensors, such as Rogowski coil, gradiometer sensors, vibrating coil sensors, tangential field sensors and needle probes are described. The applications of coil sensors as magnetic antennae are also presented.

**Keywords:** coil sensor, magnetic field measurement, search coil, Rogowski coil, vibrating coil, gradiometer, integrator circuit, H-coil sensor, needle probe method.

(Some figures in this article are in colour only in the electronic version)

## 1. Introduction

Induction coil sensors [1–4] (also called search coil sensors, pickup coil sensors, magnetic antennae) are one of the oldest and most well-known types of magnetic sensors. Their transfer function  $V = f(B)$  results from the fundamental Faraday's law of induction

$$V = -n \cdot \frac{d\Phi}{dt} = -n \cdot A \cdot \frac{dB}{dt} = -\mu_0 \cdot n \cdot A \cdot \frac{dH}{dt} \quad (1)$$

where  $\Phi$  is the magnetic flux passing through a coil with an area  $A$  and a number of turns  $n$ .

The operating principles of coil sensors are generally known but the technical details and practical implementation of such devices are only known to specialists. For example, it is well known that the output signal,  $V$ , of a coil sensor depends on the rate of change of flux density,  $dB/dt$ , which requires integration of the output signal. However, there are other useful methods which enable the obtaining of results proportional to flux density,  $B$ .

It is widely known, and evident from equation (1), that a large coil sensitivity can be obtained by using a large number of turns  $n$  and large active area  $A$ . However, the optimization process for coil performance, in many cases, is not as easy.

The properties of a coil sensor were described in detail many years ago [5]. However, sensors based on the same

operating principle are still widely used in many applications, especially for the detection of stray magnetic fields (potentially dangerous for health). The induction sensor is practically the only one that can be manufactured directly by a user (in comparison to Hall, magnetoresistive or fluxgate-type sensors). The method of coil manufacture is simple and the materials (winding wire) are commonly available. Thus, almost everyone can perform such investigations using simple and very low-cost, yet accurate, induction coil sensors.

There are many historical examples of the renaissance of various coil sensors. For example, the Chattock–Rogowski coil was first described in 1887 [6, 7]. Today, this sensor has been re-discovered as an excellent current transducer [8] and sensor used in measurement of magnetic properties of soft magnetic materials [9]. An old Austrian patent from 1957 [10] describing the use of a needle sensor (also called the stylus method) for the investigation of local flux density in electrical steel was revived several years ago for magnetic measurements [11, 12].

The main goal of this review is to summarize the existing knowledge about induction coil sensors, including old, often forgotten publications as well as new developments. Firstly, two main designs of coil sensor (with air cores and ferromagnetic cores) are described. Then, their frequency response is analysed taking into account the type of sensor and their associated output electronics. Secondly, particular

induction sensors are discussed and this is followed by a description of the most common application of this type of transducer: magnetic antennae. Finally, the main advantages and disadvantages of these sensors are discussed.

## 2. Air coils versus ferromagnetic core coils

The relatively low sensitivity of an air coil sensor and problems with its miniaturization can be partially overcome by the incorporation of a ferromagnetic core, which acts as a flux concentrator inside the coil. For a coil with a ferromagnetic core, equation (1) can be rewritten as

$$V = -\mu_0 \cdot \mu_r \cdot n \cdot A \cdot \frac{dH}{dt}. \quad (2)$$

Modern soft magnetic materials exhibit a relative permeability,  $\mu_r$ , larger than  $10^5$ , so this can result in a significant increase of the sensor sensitivity. However, it should be taken into account that the resultant permeability of the core,  $\mu_c$ , can be much lower than the material permeability. This is due to the demagnetizing field effect defined by the demagnetizing factor  $N$ , which is dependent on the geometry of the core

$$\mu_c = \frac{\mu_r}{1 + N \cdot (\mu_r - 1)}. \quad (3)$$

If the permeability  $\mu_r$  of a material is relatively large (which is generally the case) the resultant permeability of the core  $\mu_c$  depends mainly on the demagnetizing factor  $N$ . Thus, in the case of a high permeability material, the sensitivity of the sensor depends mostly on the geometry of the core.

The demagnetizing factor  $N$  for an ellipsoidal core depends on the core length  $l_c$  and core diameter  $D_c$  according to an approximate equation

$$N \cong \frac{D_c^2}{l_c^2} \cdot \left( \ln \frac{2l_c}{D_c} - 1 \right). \quad (4)$$

It can be derived from equation (4) that in order to obtain a small value of  $N$  (and a large resultant permeability  $\mu_c$ ) the core should be long and with small diameter. Let us consider the dimensions of a search coil sensor optimized for a large sensitivity as described in [13]. The core was prepared from amorphous ribbon (Metglas 2714AF) with dimensions  $l_c = 300$  mm and  $D_c = 10$  mm (aspect ratio equal to 30). Substituting these values into equation (4) we obtain  $N \cong 3.5 \times 10^{-3}$  which means that the sensitivity is about 300 times larger in comparison with the air-coil sensor.

Therefore, the use of a core made of a soft magnetic material leads to a significant improvement of the sensor sensitivity. However, this enhancement is achieved with the sacrifice of one of the most important advantages of the air-coil sensor—the linearity. The core, even if made from the best ferromagnetic material, introduces to the transfer function of the sensor some nonlinear factors which depend on temperature, frequency, flux density, etc. Additional magnetic noise (e.g. Barkhausen noise) also decreases the resolution of the sensor. Moreover, the ferromagnetic core alters the distribution of the investigated magnetic field (or flux density), which can have important consequences.



**Figure 1.** The simplest coil-based sensor for flux density and magnetic fields.

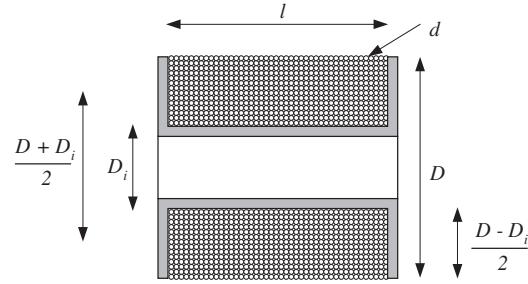


**Figure 2.** Typical design of an air coil sensor ( $l$ —length of the coil,  $D$ —outer diameter of the coil,  $D_i$ —inner diameter of the coil,  $d$ —diameter of the wire).

## 3. Design of the air-coil sensor

A typical design of an air-coil sensor is presented in figure 2. The resultant area of a multilayer coil sensor can be calculated using integration [5]

$$A = \frac{\pi}{4} \cdot \frac{1}{D - D_i} \cdot \int_{D_i}^D (y^2) dy = \frac{\pi}{12} \cdot \frac{D^3 - D_i^3}{D - D_i}. \quad (5)$$

However, equation (5) is of limited accuracy. Thus, in practice, it is better to determine the resultant area of the coil experimentally by means of calibration in a known field. The area of the coil can be calculated with a simplified formula based on the assumption that its diameter is equal to mean value  $D_m = (D + D_i)/2$ , thus

$$A = \frac{\pi}{8} \cdot (D + D_i)^2. \quad (6)$$

If we assume that the flux density to be measured is a sine wave  $b = B_m \cdot \sin(\omega \cdot t)$ , and the sensing coil is a ring with diameter  $D$ , then the relation (1) can be rewritten in a form

$$V = 0.5 \cdot \pi^2 \cdot f \cdot n \cdot D^2 \cdot B, \quad (7)$$

where  $f$  is a frequency of the measured field,  $n$  and  $D$  are number of turns and diameter of the coil, respectively and  $B$  is the measured flux density.

If we would like to determine the magnetic field strength  $H$  instead of flux density  $B$ , then the equation (7) can be easily transformed knowing that for a non-ferromagnetic medium  $B = \mu_0 \cdot H$  ( $\mu_0 = 4 \cdot \pi \cdot 10^{-7}$  H m<sup>-1</sup>) and

$$V = 2 \times 10^{-7} \cdot \pi^3 \cdot f \cdot n \cdot D^2 \cdot H. \quad (8)$$

Taking into account (6), equation (8) can be presented as

$$V = \frac{10^{-7}}{2} \cdot \pi^3 \cdot f \cdot n \cdot (D + D_i)^2 \cdot H. \quad (9)$$

The number of turns depends on the diameter,  $d$ , of the wire that is used, the packing factor  $k$  ( $k \approx 0.85$  [1]) and the dimensions of the coil

$$n = \frac{l \cdot (D - D_i)}{2 \cdot k \cdot d^2}. \quad (10)$$

Thus, the sensitivity  $S = V/H$  of an air-coil sensor can be calculated as

$$S = \frac{10^{-7}}{4} \cdot \frac{\pi^3 \cdot f \cdot l}{k d^2} \cdot (D - D_i) \cdot (D + D_i)^2. \quad (11)$$

The resolution of the coil sensor is limited by thermal noise,  $V_T$ , which depends on the resistance  $R$  of the coil, the temperature  $T$ , the frequency bandwidth  $\Delta f$  with coefficient equal to the Boltzmann factor  $k_B = 1.38 \times 10^{-23} \text{ W s K}^{-1}$

$$V_T = 2\sqrt{k_B \cdot T \cdot \Delta f \cdot R}. \quad (12)$$

The resistance of the coil can be calculated as [14]

$$R = \frac{\rho \cdot l}{d^4} (D - D_i) \cdot (D + D_i) \quad (13)$$

and the signal-to-noise ratio, SNR, of the air-coil sensor is

$$\text{SNR} = \frac{\pi^3 \cdot 10^{-7}}{8} \cdot \frac{f}{\sqrt{\Delta f}} \cdot \frac{\sqrt{l} \cdot (D + D_i) \cdot \sqrt{D^2 - D_i^2} \cdot H}{\sqrt{k^2 \cdot k_B \cdot T \cdot \rho}} \quad (14)$$

As can be seen from equation (14), the sensitivity increases roughly proportionally to  $D^3$  and SNR increases with  $D^2$ , so the best way to obtain maximal sensitivity and resolution is to increase the coil diameter  $D$ . Increasing the coil length is less effective, because the sensitivity increases with  $l$ , while the SNR increases only with  $\sqrt{l}$ . The sensitivity can also be improved by an increase in the number of turns. For example, by using wire with smaller diameter the sensitivity increases with  $d^2$  and the SNR ratio does not depend on the wire diameter.

Various publications discussed other geometrical factors of the air-coil sensor. For instance, the optimum relation between the length and the diameter of the coil can be determined taking into account the error caused by the inhomogeneous field. It was found [5, 15] that for  $l/D = 0.866$  undesirable components are eliminated at the centre of the coil. This analysis was performed for the coil with one layer. For a multilayer coil the recommended relation is  $l/D = 0.67\text{--}0.866$  (0.67 for  $D_i/D = 0$  and 0.866 for  $D_i/D = 1$ ). The same source [5] recommends  $D_i/D$  to be less than 0.3.

It can be concluded from the analysis presented above that in order to obtain high sensitivity, the air-coil sensor should be very large. For instance, the induction coil magnetometer used for measurements of micropulsations of the Earth's magnetic field in the bandwidth of 0.001–10 Hz with resolution 1 pT–1 nT [16] have metre-range dimensions and even hundreds of kilograms in weight. An example of a design of such a coil sensor for such a purpose is presented in [17]. Here a coil with diameter 2 m (16 000 turns of copper wire 0.125 mm in diameter) detected micropulsation of flux density in the bandwidth of 0.004–10 Hz. For the 1 pT field the output signal was about 0.32  $\mu\text{V}$ , whilst the thermal noise level was about 0.1  $\mu\text{V}$ .

The air-coil sensor with 10 000 turns and diameter 1 m was used to detect the flux density of the magnetic field in the pT range for magnetocardiograms [18].

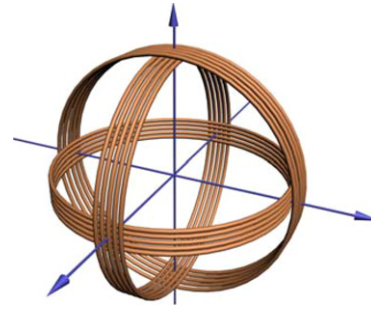


**Figure 3.** The concept of three mutually perpendicular coils for three-axis magnetic field measurements.

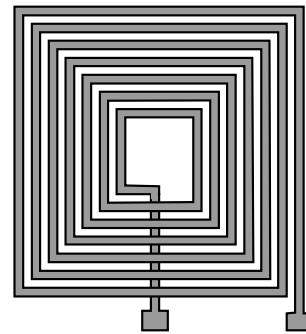


**Figure 4.** An example of a pickup planar thin film coil designed for eddy-current sensors [21].

Coil sensors are sensitive only to the flux that is perpendicular to their main axis. Therefore, in order to determine all directional components of the magnetic field vector, three mutually perpendicular coils should be used (figure 3). An example of such a low-noise three-axis search coil magnetometer is described in [19]. Such a ‘portable’ magnetometer consists of three coils of between 19 cm and 33 cm in diameter and 4100–6500 turns with a weight of 14 kg. It is capable of measuring the magnetic field between 20 Hz and 20 kHz with a noise level lower than 170 dB/100  $\mu\text{T}$ .

On the other hand, there are examples of extremely small air-cored sensors. Three orthogonal coil systems with dimensions less than 2 mm and a weight about 1 mg (40 turns) have been used for the detection of position of small, fast moving animals [20].

Air-coil sensors are widely used as eddy-current proximity sensors or for eddy-current sensors for non-destructive testing (e.g. for detection of cracks). In such cases, sensitivity is not as important as the spatial resolution and compactness of the whole device. Such sensors are often manufactured as a flat planar coil (made in PCB or thin film technology [21–25]) connected to an on-chip CMOS electronic circuit [22]. An example of such a sensor with dimensions of  $400 \times 400 \mu\text{m}^2$  (7 turns) is presented in figure 4.

For testing the spatial distribution of the magnetic field by means of coil sensors the flexible microloop sensor array has been developed [26]. The array consists of 16 microloop sensors with an area of  $14 \times 14 \text{ mm}^2$  and a thickness of 125  $\mu\text{m}$ . Each coil has 40 turns within an area of  $2 \times 2 \text{ mm}^2$ .

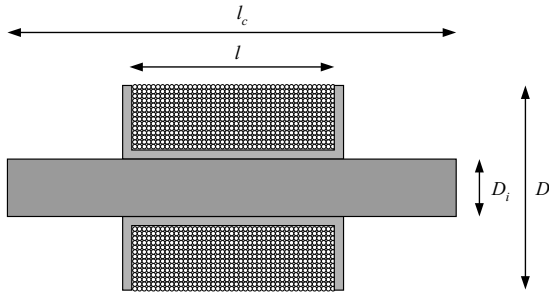


**Figure 5.** Design of a typical ferromagnetic core coil sensor ( $l$ —length of the coil,  $l_c$ —length of the core,  $D$ —diameter of the coil,  $D_i$ —diameter of the core).

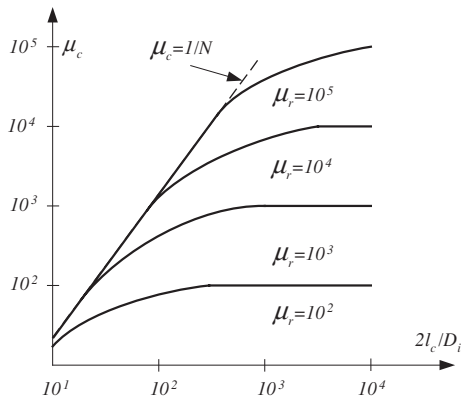


**Figure 6.** The dependence of the resultant permeability of the core on the dimensions of the core and the permeability of the material [14].

Sometimes, the frequency response of the air-core sensor is a more important factor than the sensitivity or spatial resolution. The dimensions of the coil can be optimized for better frequency performance. These factors are discussed in section 5.

#### 4. Design of ferromagnetic core coil sensor

High-permeability core coil sensors are often used in the case when high sensitivity or dimension limitations are important. A typical geometry of such a sensor is presented in figure 5.

The optimal value of core diameter  $D_i$  has been determined as  $D_i \cong 0.3 D$  [14]. The length of the coil  $l$  is recommended to be about  $0.7$ – $0.9 l_c$ . For such coil dimensions, the output signal  $V$  and SNR ratio at room temperature can be described as [27]

$$V \cong 0.9 \times 10^{-5} \cdot f \cdot \frac{l^3}{d^2} \cdot D_i \cdot \frac{1}{\ln(2 \cdot l/D_i) - 1} \cdot H \quad (15)$$

$$\text{SNR} \cong 1.4 \times 10^8 \cdot \frac{f}{\sqrt{\Delta f}} \cdot l^2 \cdot \sqrt{l} \cdot \frac{1}{\ln(2 \cdot l/D_i) - 1} H \quad (16)$$

It can be concluded from relationships (15) and (16) that in the case of a coil sensor with a ferromagnetic core the most efficient method of improving the sensor performance is to make the length of the core (or rather the ratio  $l/D_i$ ) as large as possible, since the sensitivity is proportional to  $l^3$ . Figure 6 presents the dependence of the resultant permeability

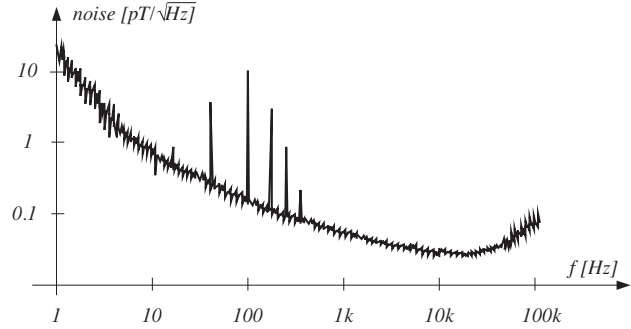


**Figure 7.** An example of the noise performance of the induction magnetometer (after [28]).

of the core  $\mu_c$  on the aspect ratio  $l/D$  and the core material permeability  $\mu_r$  (as described in [14]).

The choice of the aspect ratio of the core is very important. The length should be sufficiently large to benefit from the permeability of the core material. On the other hand, if the aspect ratio is large the resultant permeability depends on the material permeability. This may cause error resulting from the instability of material permeability due to the changes of temperature or applied field frequency. For large values of material permeability the resultant permeability  $\mu_c$  practically does not depend on material characteristics because relation (3) is then

$$\mu_c \approx \frac{1}{N}. \quad (17)$$

Higher values of material permeability allow the use of longer cores without the risk of the resultant permeability depending on the magnetic characteristic of the material used.

As an example, let us consider a low-noise induction magnetometer that is described in [28]. Here, the core was prepared from amorphous ribbon (Metglas 2714AF) with temperature-independent properties and dimensions: length 150 mm, cross-section of the order  $5 \times 5 \text{ mm}^2$  (aspect ratio of around 27). A coil of 10 000 turns was wound with a 0.15 mm diameter wire. The noise characteristic of this sensor is presented in figure 7. The obtained noise level around  $0.05 \text{ pT Hz}^{-1/2}$  was found to be comparable with the values reported for SQUID sensors.

The same authors compared the influence of the core material. For an amorphous Metglas core the noise was found to be  $0.05 \text{ pT Hz}^{-1/2}$ , whilst for the same sensor with a permalloy Supermetal core it exhibited larger noise of  $2 \text{ pT Hz}^{-1/2}$ . Also, a comparison of air coil and ferromagnetic core sensors has been reported [29, 30]. Experimental results show that well-designed ferromagnetic core induction sensors exhibited a linearity comparable with air-core sensors.

Sensors with ferromagnetic cores are often used for magnetic investigations in space research [31, 32]. Devices with a core length of 51 cm and weight of 75 g (including preamplifier) exhibited a resolution (noise level) of  $2 \text{ fT Hz}^{-1/2}$  [33]. In an analysis of Earth's magnetic field (OGO search coil experiments) the following three-axis sensors have been used: coil 100 000 turns of 0.036 mm in diameter, core made from nickel-iron alloy 27 cm long and square ( $0.6 \times 0.6 \text{ cm}^2$ ) cross-section. Each sensor weighted 150 g (with half

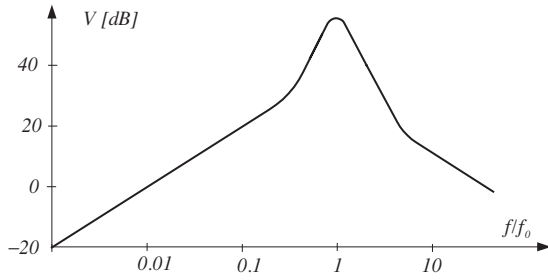


**Figure 8.** Typical frequency characteristic of an induction coil sensor.

the weight being the core). The sensitivity in this case was  $10 \mu\text{V} (\text{nT Hz})^{-1}$  [34].

The detailed design and optimization of an extremely sensitive three-axis search coil magnetometer for space research is described in [35]. The coil magnetometer developed for the scientific satellite DEMETER had a noise level of  $4 \text{ fT Hz}^{-1/2}$  at 6 kHz. To obtain the desired resonance frequency and a resistance noise above the preamplifier voltage noise the diameter of copper wire of  $71 \mu\text{m}$  and number of turns of 12 200 were selected. The core was built from 170 mm long  $50 \mu\text{m}$  thick annealed FeNiMo 15–80–5 permalloy strips, with a cross section of  $4.2 \text{ mm} \times 4.2 \text{ mm}$ . The mass of the whole three-axis sensor and the bracket was only 430 g.

There are commercially available search coil sensors. For example, MEDA Company offers sensors with a sensitivity of  $25 \text{ mV nT}^{-1}$  and noise at 10 kHz equal to  $10 \text{ fT Hz}^{-1/2}$  (MGCH-2 sensor with a core length about 32 cm) or at 0.2 Hz equal to  $2.5 \text{ pT Hz}^{-1/2}$  (MGCH-3 sensor with a core length of about 1 m) [36].

## 5. Frequency response of search coil sensors

It is obvious from equation (1) that in order to obtain any output voltage signal from the sensor the flux density must be varying with time. Therefore, the coil sensors are capable of measuring only dynamic (AC) magnetic fields. In the case of the dc magnetic fields the variation of the flux density can be ‘forced’ in the sensors by moving the coil. However, the term ‘dc magnetic field’ can be understood as a relative one. By using a sensitive amplifier and a large coil sensor it is possible to determine low-frequency (mHz) magnetic fields [16, 17]. Thus, it is also possible to investigate quasi-static magnetic fields with fixed-coil (unmovable) sensors.

AC magnetic fields with a frequency up to several MHz can be investigated by means of coil sensors [37]. In special designs, this bandwidth can be extended to GHz range [38, 39]. An example of the typical frequency characteristic of a coil sensor is presented in figure 8.

According to (7) the output signal depends linearly on frequency, but due to the internal resistance  $R$ , inductance  $L$  and self-capacitance  $C$  of the sensor, the dependence  $V = f(f)$  is more complex. The equivalent electric circuit of an induction sensor is presented in figure 9.

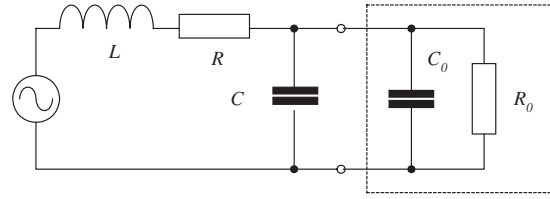


**Figure 9.** Equivalent circuit of induction sensor loaded with capacity  $C_0$  and resistance  $R_0$ .

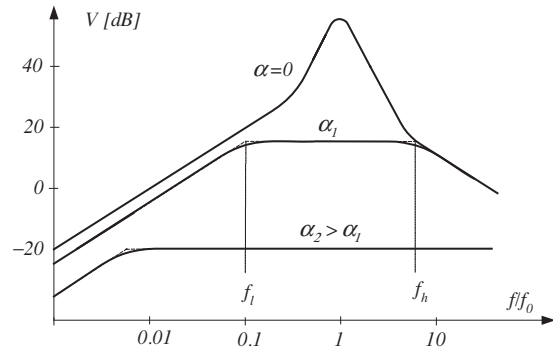


**Figure 10.** Frequency characteristics of the induction coil loaded by the resistance  $R_0$  (the coefficient  $\alpha = R/R_0$ ).

The output signal increases, initially almost linearly with the frequency of measured field, up to resonance frequency

$$f_0 = \frac{1}{2 \cdot \pi \cdot \sqrt{L \cdot C}}. \quad (18)$$

Above the resonance frequency the influence of self-capacitance causes the output signal to drop.

Analysing the equivalent circuit of the sensor, the sensitivity  $S = V/H$  can be expressed in the form [40]

$$S = \frac{S_0}{\sqrt{(1 + \alpha)^2 + \left(\beta^2 + \frac{\alpha^2}{\beta^2} - 2\right) \cdot \gamma^2 + \gamma^4}}, \quad (19)$$

where  $\alpha = R/R_0$ ,  $\beta = R \cdot \sqrt{C/L}$ ,  $\gamma = f/f_0 = 2 \cdot \pi \cdot f \cdot \sqrt{L \cdot C}$ .

The absolute sensitivity  $S_0$  can be described as  $S_0 = 2 \times 10^{-7} \cdot \pi^3 \cdot n \cdot D^2$ . The graphical form of the relation (19) is presented in figure 10.

The sensor loaded with a small resistance  $R_0$  exhibits a frequency characteristic with a plateau between the low corner frequency

$$f_i = \frac{R + R_0}{2 \cdot \pi \cdot L} \quad (20)$$

and the high corner frequency

$$f_h = \frac{1}{2 \cdot \pi \cdot R_0 \cdot C}. \quad (21)$$

A frequently used method for the improvement of the sensor frequency characteristic is the connection of an integrating transducer to the sensor output. Another method is a load of a sensor with a very low resistance (current-to-voltage converter). For low value of load resistance  $R_0$  (high value of  $\alpha$  coefficient—see figure 10) we can operate on the plateau of frequency characteristic (in the so-called self-integration mode).

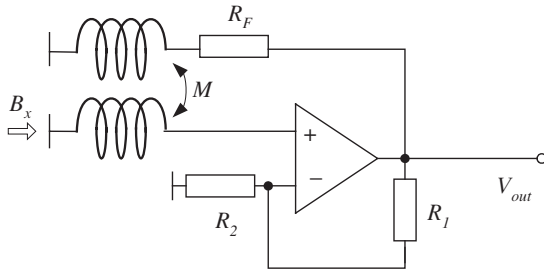


**Figure 11.** Induction coil sensor connected to the amplifier with negative transformer type feedback.

The inductance of the sensor depends on the number of turns, permeability and the core dimensions, according to the following empirical formula [40]:

$$L = n^2 \cdot \frac{\mu_0 \cdot \mu_c \cdot A_c}{l_c} \cdot \left(\frac{l}{l_c}\right)^{-3/5} \quad (22)$$

The self-capacitance of the sensor strongly depends on the construction of the coil (the application of the shield between the coil layers significantly changes the capacitance).

The frequency characteristic below  $f_l$  can be additionally improved by incorporating a PI correction circuit (more details are given in the next section).

A feedback circuit is another method of improvement of the frequency characteristic of the sensor [4, 41, 42] as presented in figure 11.

The output signal of the circuit presented in figure 11 can be described as [41]

$$V_{out} = 2 \cdot \pi \cdot f \cdot n \cdot \mu_0 \cdot \mu_c \cdot A_c \cdot \frac{R_F}{2 \cdot \pi \cdot M} \cdot \frac{j \cdot \omega / \omega_l}{1 + j \cdot \omega / \omega_l} \cdot \frac{1}{1 + j \cdot \omega / \omega_h} \cdot B_x \quad (23)$$

The circuit described by equations (23) represents a high-pass filter working under  $\omega \ll \omega_0$ , and a low-pass filter for  $\omega \gg \omega_0$ . As a result, the frequency characteristic is flat between low

$$\omega_l = \frac{R_F}{M} \cdot \frac{1}{1 + R_1/R_2} \quad (24)$$

and high frequency

$$\omega_h = \frac{1 + R_1/R_2}{R_F} \cdot M \cdot \omega_0 \quad (25)$$

When improvement of the low-frequency characteristic due to the feedback is not sufficient, additional suppression of low-frequency noise is possible by introduction of RC-filters, as is proposed in [43].

The air-core sensors, due to their relatively low inductance, are used as large frequency bandwidth current transducers (in the Rogowski coil configuration described later) typically up to 1 MHz with an output integrator and up to 100 MHz with current-to-voltage output.

## 6. Electronic circuits connected to the coil sensors

Because the output signal of an induction coil is dependent on the derivative of the measured value ( $dB/dt$  or  $dI/dt$  in the case of a Rogowski coil) one of the methods of recovering the

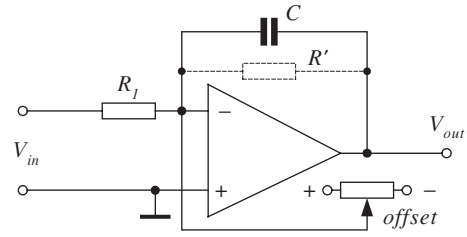


**Figure 12.** Typical integrating circuit for the coil signal.

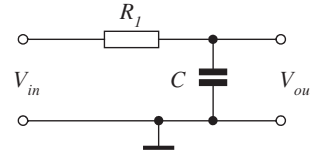


**Figure 13.** The passive integrating circuit.

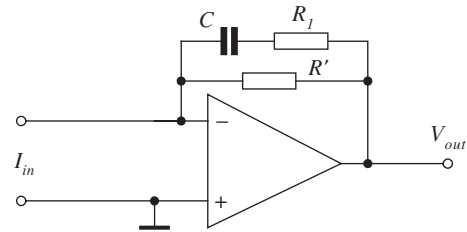


**Figure 14.** Current-to-voltage transducer with additional frequency correction circuit. An example described in [28] with elements:  $R_1 = 100 \text{ k}\Omega$ ,  $C = 0.22 \text{ }\mu\text{F}$ ,  $R' = 47 \text{ M}\Omega$ .

original signal is the application of an integrating transducer [44] (figure 12).

Figure 12 presents a typical analogue integrating circuit. The presence of the offset voltage and associated zero drift are a significant problem in the correct design of such transducers. For this reason, an additional potentiometer is sometimes used for offset correction and resistor  $R'$  is introduced for the limitation of the low-frequency bandwidth. The output signal of the integrating transducer is

$$V_{out} = -\frac{1}{R \cdot C} \cdot \int_{t_0}^{T+t_0} (V_{in}) dt + V_0, \quad (26)$$

where  $R = R_1 + R_{coil}$ . The resistance  $R$  should be sufficiently large (as not to load the coil) as well as the capacitance  $C$ —typical values are  $R_1 = 10 \text{ k}\Omega$  and  $C = 10 \text{ }\mu\text{F}$  [44].

The amplifier can introduce several limitations at higher frequencies. A passive integrating circuit (figure 13) exhibits somewhat better performance at those frequencies. Combinations of various methods of integration (active and passive) can be used for large bandwidth—as proposed in [45].

Problems with the correct design of a measuring system with an integrating transducer are often overcome by applying low resistance loading to the coils (self-integration mode presented in figure 10). Usually, a current-to-voltage converter is used as an output transducer, additionally supported by a low-frequency correction circuit. An example of such a transducer is presented in figure 14.

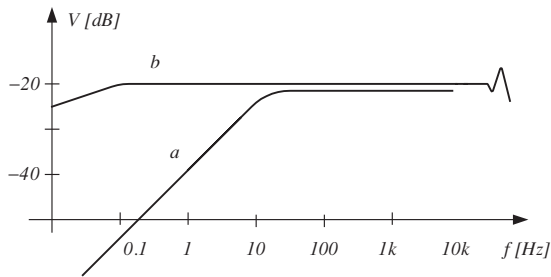


**Figure 15.** Frequency characteristic of a coil sensor with current-to-voltage transducer (a) and with additional correction circuit (b).

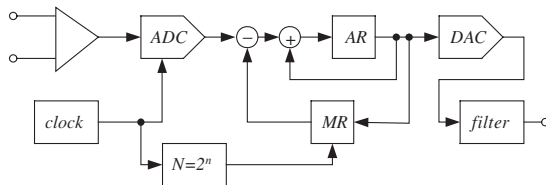


**Figure 16.** Digital transducer of the coil sensor signal (after [48]).

In the current-to-voltage transducer presented in figure 14 the correction circuit  $R_1C$  is introduced to correct the characteristic of a low-resistance loaded circuit at lower frequencies, as illustrated in figure 15.

The above-described circuits were equipped with analogue transducers at the output of the coil sensor. However, it is also possible to convert the output signal to a digital form and then to perform digital integration—several examples of such approaches (with satisfactory results) have been described in [46–48].

Accurate digital integration of the coil sensor signal is not a trivial task. Also, in digital processing there are integration zero drifts. The most frequently used method eliminating this problem is the subtraction of the calculated average value of the signal. The integrating period, sampling frequency and triggering time should be carefully chosen, especially when the exact frequency of the processed signal is unknown (which is often the case). Moreover, the cost of a good quality data acquisition circuit (analogue-to-digital converter) is relatively high and the use of a PC is necessary. Therefore, in some cases the integrating process is performed digitally by relatively simple hardware (without a PC), consisting of analogue-to-digital (ADC) and digital-to-analogue (DAC) circuits and registers (AR and MR) as is presented in figure 16.

It is worth noting that almost all companies manufacturing the equipment for magnetic measurements (such as Brockhaus, LakeShore, Magnet Physik, Walker Scientific) offer digital integrator instruments, called Fluxmeters—often equipped with coil sensors. Figure 17 presents the coil sensor used in this instrument.

The amplifier connected to the coil sensor introduces additional noise, voltage noise and current noise, as illustrated in figure 18. Each noise component is frequency dependent. Analysis of the coil sensor connected to the amplifier [1] indicates that for low frequency the thermal noise of the sensor dominates. Above the resonance frequency the amplifier noise dominates.

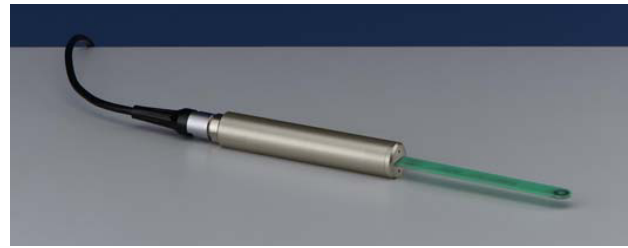


**Figure 17.** An example of the coil sensor used in a digital fluxmeter of Brockhaus.

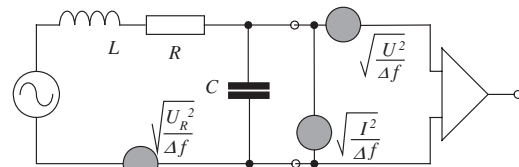


**Figure 18.** The sources of the noise in the equivalent circuit of the coil connected to the amplifier.

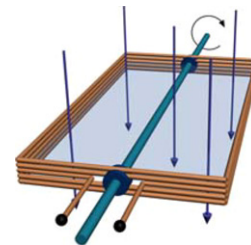


**Figure 19.** The sensor of a dc magnetic field with a rotating coil.

The reduction of the amplifier noise can be achieved by the application of a HTS SQUID picovoltmeter, as it has been reported in [48]. Indeed, the noise level of the preamplifier was decreased to a level of  $110 \text{ pV Hz}^{-1/2}$ , but the dynamic performances of such a circuit deteriorated.

## 7. Special kinds of induction coil sensors

### 7.1. Moving coil sensors

One of the drawbacks of the induction coil sensor, the sensitivity only to varying magnetic fields, can be overcome by introducing movement to the coil. For example, if the coil rotates (figure 19) with quartz-stabilized speed rotation it is possible to measure dc magnetic fields with very good accuracy. The main condition of the Faraday's law (the variation of the flux) is fulfilled, because the sensor area varies as  $a(t) = A \cdot \cos(\omega \cdot t)$  and the induced voltage is

$$V = -B_x \cdot n \cdot A \cdot \sin(\omega \cdot t). \quad (27)$$

Instead of rotation it is possible to move the sensor in other ways, the most popular being a vibrating coil. One of the first such ideas was applied by Groszkowski, who in 1937 demonstrated the moving coil magnetometer [50]. The coil was forced to vibrate by connecting it to a rotating eccentric wheel.

One of the best excitation methods for vibrating a coil is by connecting it to an oscillating element, such as a piezoelectric

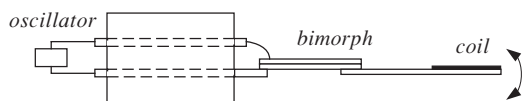


**Figure 20.** The vibrating cantilever magnetic field sensor (after [52]).

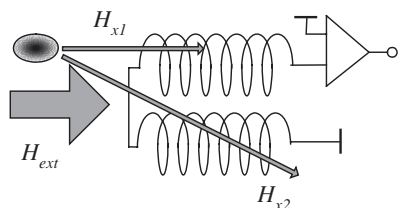


**Figure 21.** Operating principle of gradiometer sensor.

ceramic plate [51, 52]. Due to a relatively high frequency of vibration (in the kHz range) it is possible to make a very small sensor with a relatively good geometrical resolution. Figure 20 presents an example of a pickup coil sensor mounted onto a piezoelectric bimorph cantilever. The ten-turn coil, 30  $\mu\text{m}$  wide and 0.8  $\mu\text{m}$  thick, excited to a vibration frequency of around 2 kHz (mechanical resonance frequency) exhibited a sensitivity of around 18  $\mu\text{V}/100 \mu\text{T}$  [52].

It is also possible to perform measurements by quick removal of the coil sensor from a magnetic field (or quick insertion into a magnetic field). Such extraction coil methods (with the application of a digital fluxmeter with a large time constant) enable the measurement of the dc magnetic field according to the following relationship [53]:

$$\int V dt = -n \cdot A \cdot (B_x - B_o). \quad (28)$$

The moving coil methods are currently rarely used, because generally there is a tendency to avoid any moving parts in measuring instruments. For measurements of dc magnetic field, Hall sensors and fluxgate sensors are most frequently used.

### 7.2. The gradiometer sensors

The gradiometer sensors (gradient sensors) are commonly used in SQUID magnetometers for the elimination of the influence of ambient fields [54]. These sensors can be also used in other applications where ambient fields disturb the measurements, or determination of the magnetic field gradient itself [55].

The operating principle of the gradiometer sensor is shown in figure 21. The external magnetic field is generated by a large and distant source (for example, the Earth’s magnetic field), so it is assumed that this field is uniform. If two coil sensors (with a small distance between them) are inserted into such a field then both will sense the same magnetic field. As both coils are connected differentially (see figure 21) the influence of the external field is eliminated. If at the same time there is a smaller source of magnetic field (e.g due to the human heart investigated in magnetocardiograms) near both of the coils, then the magnetic field in the coil placed nearer the source is larger than in the other coil. This small difference, hence

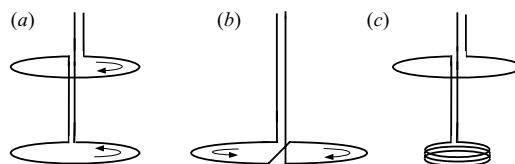


**Figure 22.** Gradiometer coils arranged: (a) vertically, (b) horizontally, (c) asymmetrically.

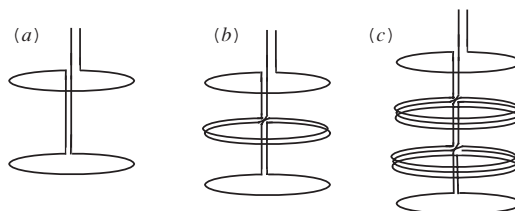


**Figure 23.** Gradiometers of a: (a) first order, (b) second order, (c) third order.

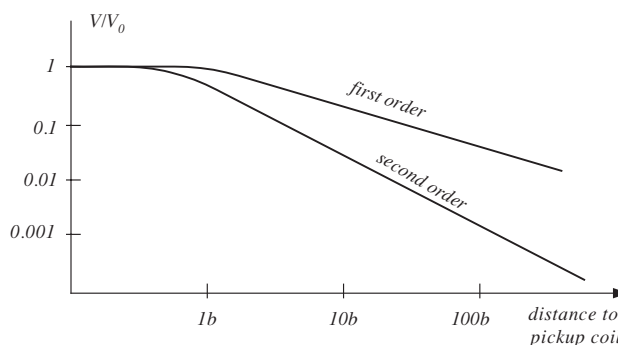


**Figure 24.** A typical response of a gradient coil sensor to the source with a distance from the pickup coil smaller than 0.3b (b being the distance between coils of gradiometer) (after [56]).

the gradient of the magnetic field, is therefore detected by the gradiometer sensor. In this way it is possible to measure a relatively small magnetic field from a local source in the presence of a much larger magnetic field from a distant one.

Figure 22 presents typical arrangements of the gradiometer coils: vertical, planar and asymmetric. A well-designed gradiometer coil should indicate zero output signal when inserted into a uniform field. In the asymmetric arrangement the sensing coil is smaller, hence has more turns in order to compensate the magnetic field detected by the larger coil.

It is possible to improve the ability to reject the common component by employing several gradiometers. Figure 23 presents first-order, second-order (consisting of two gradiometers of first order) and third-order gradiometers.

Figure 24 presents a typical response of the gradiometer coils to a source distant from the sensor [56]. The first-order gradiometer rejects more than 99% of the source at a distance of 300b (where b is the distance between the single coils of the gradiometer). For the second-order gradiometer this distance is diminished to about 30b. It is possible to arrange even higher order of the gradiometer (figure 23(c) presents

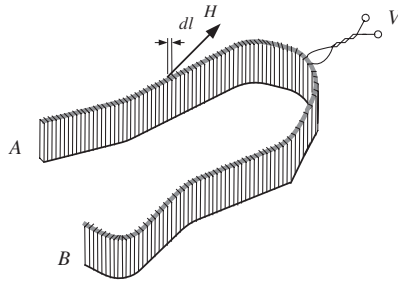


**Figure 25.** An example of a Rogowski coil (A, B—ends of the coil).

the gradiometer of the third order), but gradiometers of higher order have reduced sensitivity and SNR ratio.

The quality of the gradiometer sensor is often described by the formula

$$V \propto G + \beta \cdot H, \quad (29)$$

where  $G$  is the gradient of the measured field and  $H$  is the magnitude of the uniform field. In superconducting devices it is possible to obtain a  $\beta$  factor as small as part-per-million. This means that it is possible to detect magnetic fields of tens of femtotesla in the presence of a millitesla uniform ambient field.

### 7.3. The Rogowski coil

The special kind of helical coil sensor uniformly wound on a relatively long non-magnetic circular or rectangular strip, usually flexible (figure 25), is commonly known as the Rogowski coil, after the description given by Rogowski and Steinhaus in 1912 [5]. Sometimes this coil is called a Chattock coil (or Rogowski–Chattock potentiometer, RCP). Indeed, the operating principle of such a coil sensor was first described by Chattock in 1887 [6] (it is not clear if Rogowski knew the disclosure of Chattock, because in Rogowski's article Chattock was not cited).

The induced voltage is used as the output signal of the Rogowski coil. But the principle of operation of this sensor is based on Ampere's law rather than Faraday's law. If the coil of length  $l$  is inserted into a magnetic field then the output voltage is the sum of voltages induced in each turn (all turns are connected in series)

$$\begin{aligned} V &= \sum \left( -n \cdot \frac{d}{dl} \cdot \frac{d\phi}{dt} \right) \\ &= \mu_0 \cdot \frac{n}{l} \cdot A \cdot \frac{d}{dt} \cdot \int_A^B (H) dl \cdot \cos(\alpha). \end{aligned} \quad (30)$$

The output signal of the Rogowski coil depends on the number of turns per unit length  $n/l$  and the cross section area,  $A$ , of the coil. A correctly designed and manufactured Rogowski coil inserted in the magnetic field at fixed points A–B should give the same output signal independent of the shape of the coil between the points A and B. A coil with connected ends (length A–B equal to zero) should have zero output signal.

One of the important applications of the Rogowski–Chattock coil is the coil in the device for testing of magnetic materials known as a SST (single sheet tester) [8, 57, 58]. In such a device it is quite difficult to use Ampere's law ( $H \cdot l =$

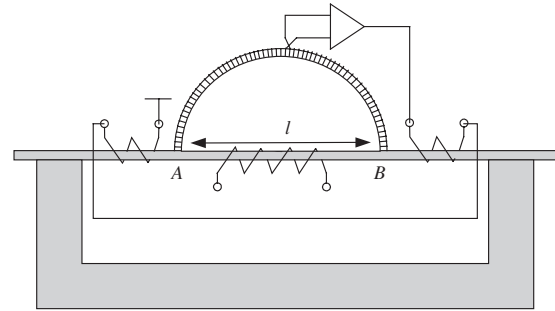


**Figure 26.** The application of a Rogowski coil for the determination of  $H \cdot l$  value.

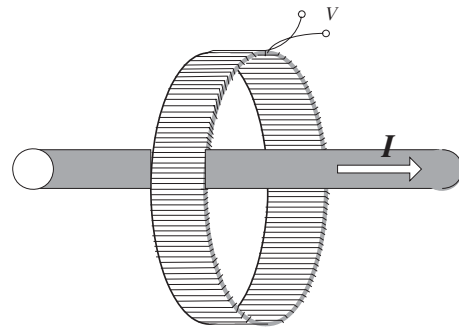


**Figure 27.** The Rogowski coil as a current sensor.

$I \cdot n$ ) for the determination of the magnetic field strength  $H$  (from the magnetizing current  $I$ ), because the mean length  $l$  of the magnetic path is not exactly known (in comparison to a closed circuit system). But if the RCP coil is used we can assume that the output signal of this coil is proportional to the magnetic field strength between the points A–B

$$V = \mu_0 \cdot \frac{n}{l} \cdot A \cdot \frac{d}{dt} (H \cdot l_{AB}). \quad (31)$$

The RCP coil can be used to determine the  $H \cdot l$  value, that is the difference of magnetic potentials. The application of the coil to direct measurements of  $H$  (for fixed value of length  $l_{AB}$ ) is not convenient, because the output signal is relatively small and integration of the output voltage is required. For this reason, the compensation method shown in figure 26 is more often used. In such a method the output signal of the RCP coil is utilized as the signal for the feedback circuit for the current exciting the correction coils. Due to the negative feedback circuit the output signal of the coil is equal to zero, which means that all magnetic field components in the air gaps and the yoke are compensated and

$$H \cdot l_{AB} - n \cdot I = 0. \quad (32)$$

Thus, the magnetic field strength can be determined directly from the magnetizing current because the other parameters ( $l_{AB}$  and  $n$ ) are known.

The most important application of the Rogowski coil is for current measurements [59–63]. When the coil wraps around a current conducting wire (figure 27) the output signal of the sensor is

$$V = \mu_0 \cdot \frac{n}{l} A \cdot \frac{dI}{dt}. \quad (33)$$



**Figure 28.** An example of the Rogowski coil current sensor—model 8000 of Rocoil [68].

The Rogowski coil used as a current sensor enables measurements of very high values of current (including plasma current measurements in space [32]). Due to the relatively small inductance of such sensors they can be used to measure the transient current of pulse times down to several nanoseconds [63]. Other advantages of the Rogowski coil as a current sensor in comparison with current transformers are as follows: excellent linearity (lack of saturating core), no danger of opening the second winding of the current transformer and low construction costs. Therefore, the Rogowski current sensor in many applications has effectively substituted current transformers. The application of the Rogowski coil for current measurements is so wide that recently Analog Devices equipped the energy transducer (model AD7763) with an integrating circuit for connecting the coil current sensors.

Although the Rogowski coil seems to be relatively simple in design, careful and accurate preparation is strongly recommended to obtain the expected performance [64–66]. First, it is important to ensure the uniformity of the winding (for perfectly uniform winding the output signal does not depend on the path the coil follows around the current-carrying conductor or on the position of the conductor). Special methods and machines for the manufacture of Rogowski coils have been proposed [65–67]. The output signal, thus also the sensitivity, can be increased by increasing the area of the turn, but for correct operation (according to Ampere’s law) it is required to ensure the homogeneity of the flux in each turn. For this reason, the coil is wound on a thin strip with a small cross-sectional area. Also, the positioning of the return loop is important—both terminals should be at the same end of the coil. When the coil is wound on a coaxial cable the central conductor can be used as the return path [64].

There are several manufacturers offering various types of Rogowski coils or Rogowski coil current sensors. Figure 28 shows an example of the Rogowski coil transducer (coil and integrator transducer) of Rocoil Rogowski Coils Ltd [68].

#### 7.4. The flux ball sensor

It is quite difficult to manufacture a coil sensor with sufficient sensitivity and small dimensions for measurements of local magnetic fields. If the investigated magnetic field is inhomogeneous, then the sensor averages the magnetic field

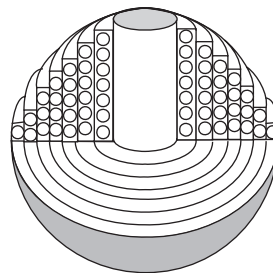


**Figure 29.** An example of a spherical coil sensor.

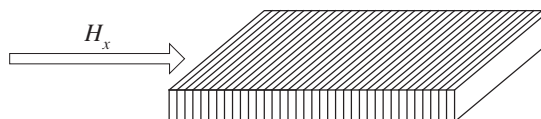


**Figure 30.** An example of a typical H-coil sensor.

over the area of the coil. Axially symmetric coils inserted into an inhomogeneous field are insensitive to all even gradients. As described in section 3, for certain coil dimensions ( $l/D \approx 0.67$ ) the odd gradients can also be eliminated.

Brown and Sweer [69] demonstrated that the volume averaging of the field over the interior of any sphere centred at a point is equal to the value of the magnetic field at this point. Thus, a spherical coil measures the field value at its centre. An example of a design of such a spherical coil sensor is shown in figure 29.

#### 7.5. Tangential field sensor (H-coil sensor)

Measurements of the magnetic field strength in magnetic materials (for example electrical steel sheet) utilize the fact that the magnetic field inside the magnetic materials is the same as the tangential field component directly above this material. Thus, a flat coil called an H-coil is often used for the measurements of the magnetic field strength [70, 71].

The coil sensor for the measurement of the tangential component should be as thin as possible. This is in conflict with the requirement for the optimum sensitivity of the sensor, which depends on the cross-section area of the coil. A typical coil sensor with a thickness of 0.5 mm and an area of 25 mm × 25 mm wound with a wire of 0.05 mm in diameter (about 400 turns) exhibits a sensitivity of around  $3 \mu\text{V} (\text{A m})^{-1}$  [72].

In order to obtain sufficient sensitivity the coil sensor is manufactured with a thickness of about 0.5 mm or more. Thus, the axis of the coil is somewhat distanced from the magnetic material surface under investigation. Nakata [71] proposed a two-coil system where the value of the magnetic field directly at the surface can be extrapolated from two results. This idea has been tested numerically and experimentally [73]. It was shown that such a method enables the determination of the magnetic field on the magnetic material surface even if the sensor is at a distance of more than 1 mm from this surface. Additionally it was proposed to enhance the two-coil method by application of up to four parallel (or perpendicular) sensors. An example of such a multi-coil sensor is shown in figure 31(b).

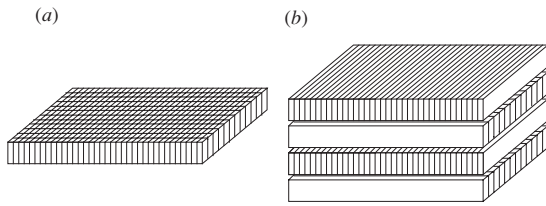


**Figure 31.** Two examples of a coil sensor for two components of magnetic field: (a) two perpendicular H-coils wound around the same former, (b) four separate coils allowing double-coil measurements.

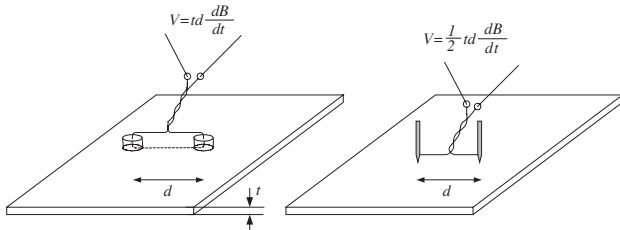


**Figure 32.** Two methods of local flux density measurements: micro-holes method and needle method.

### 7.6. The needle sensors (B-coil sensors)

When it was necessary to determine the local value of the flux density in electrical steel sheet practically only one method was available (apart from the optical Kerr method): to drill two micro-holes (with diameter 0.2–0.5 mm) and to wind one- or more-turn coil (figure 32(a)).

However, drilling such small holes in relatively hard material is not easy. Moreover, this method is destructive. In order to avoid these problems, several years ago Japanese researchers [11, 74, 75] returned to an old Austrian patent of Werner [10]. Werner proposed to form a one-turn coil by using two pairs of needles, but the application of his invention was difficult, due to relatively small (less than mV) output signal of the sensor. Experimental and theoretical analyses [11, 12, 74–78] proved that today this method can be used with satisfactory results. It is sufficient to use one pair of needles to form a half-turn coil sensor where the induced voltage is described by the following relation:

$$V \approx \frac{1}{2} \cdot t \cdot d \cdot \frac{dB}{dt}, \quad (34)$$

where  $t$  is the thickness of the steel sheet and  $d$  is the distance between the needles.

Although the needle method is not as accurate as the micro-holes method, it is widely used for flux density measurements, especially in two-dimensional testing of electrical steel sheets. To ensure correct contact with the insulated surface of the sample the needle tip should be specially prepared [78].

## 8. Coil sensor used as a magnetic antenna

Similar to other magnetic field sensors, coil sensors are often used for measurements of non-magnetic values. They are used in non-destructive testing (NDT), as proximity sensors, current sensors, reading heads etc. However, the detection of magnetic

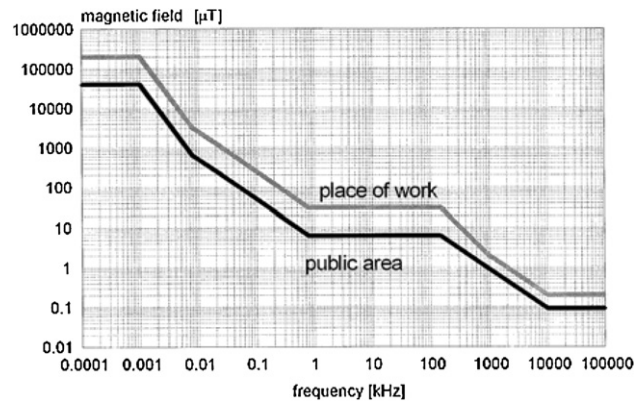


**Figure 33.** Reference levels of the magnetic field recommended by ICNIRP [79].

fields is their primary application, the importance of which is heightened due to the need for stray field investigations, especially for electromagnetic compatibility and protection against dangerous magnetic fields in the human environment.

University laboratories are often visited by ordinary people, who live near transformer stations or power transmission lines. They may wonder if such close proximity to such sources of magnetic fields can be potentially dangerous for their health, and so they have a genuine interest in the measurement of magnetic field intensities.

It is possible to do these measurements yourself. It is sufficient, for example, to wind 100 turns of a copper wire on a non-magnetic tube (5–10 cm diameter) (figure 1) and to measure the induced voltage. Then, if for instance  $f = 50$  Hz,  $n = 100$  and  $D = 10$  cm we obtain (according to relations (7) and (8)) a simple expression for output voltage:  $V$  (V)  $\cong 246.5 B$  (T) or  $V$  (V)  $\cong 0.3096 \times 10^{-3} H$  (A m<sup>-1</sup>). Of course, there are many commercially available professional measuring instruments using similar methods. Figure 33 shows the limits for exposure to time-varying magnetic fields recommended by ICNIRP (International Commission on Non-Ionizing Radiation Protection) and WHO (World Health Organization) [79].

Moreover, starting from 2006 all products indicated by the CE sign should fulfil European Standard EN 50366:2003 ‘Household and similar appliances—Electromagnetic Fields—Methods for evaluation and measurements’. Figure 34 presents the professional measuring instrument of Narda [80] designed for the determination of electromagnetic compatibility conditions according to the European Standard EN 50366.

The European Standard EN 50366 requires that the magnetic field value should be isotropic. As the coil sensor detects the magnetic field only in one direction, a three-coil system (shown in figure 3) should be used and then the value of magnetic field should be determined as

$$b(t) = \sqrt{b_x^2(t) + b_y^2(t) + b_z^2(t)}. \quad (35)$$

For investigations of magnetic pollution (magnetic smog) the author designed and constructed a magnetometer consisting of an air-coil sensor (figure 35) and amplifier/frequency correction system (figure 36). The coil was wound onto a



**Figure 34.** An example of a search coil magnetometer used for testing electromagnetic compatibility (with permission of Narda Company).



**Figure 35.** The air-coil sensor designed for investigations of magnetic pollution.

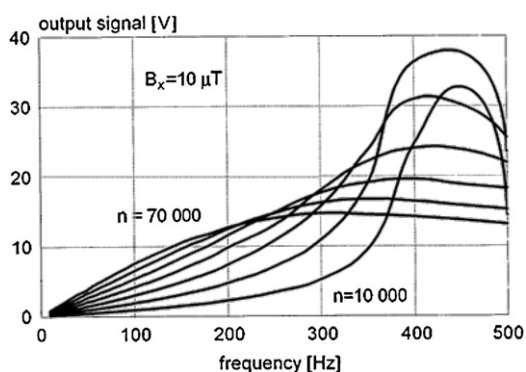


**Figure 36.** Frequency characteristics of the constructed sensor.

ring with a diameter of 60 mm and a width of 35 mm using a wire of 0.1 mm diameter. There were 70 000 turns and the coil was divided into seven sections with 10 000 turns each. The frequency characteristics of this sensor are shown in figure 36, and the summary of sensor performance is shown in table 1.

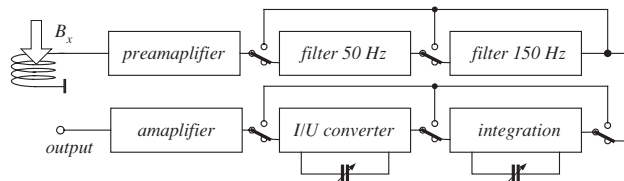


**Figure 37.** Block diagram of the induction magnetometer.

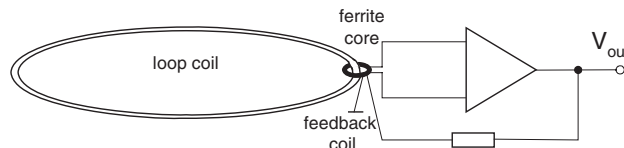


**Figure 38.** The loop sensor with feedback coil MHz range application [4].

**Table 1.** Performances of constructed sensor.

$n$	$D$ (mm)	$R$ (k $\Omega$ )	$L$ (H)	$S/f$ (mV $\mu$ T $^{-1}$ ) for 50 Hz	$f_0$ (Hz)
10 000	130	8.8	19	45	450
20 000	140	18.2	76	95	430
30 000	147	28.1	168	150	410
40 000	156	38.6	303	210	410
50 000	165	54.1	473	270	380
60 000	173	66	673	330	350
70 000	181	82	932	380	300

The block diagram of the constructed magnetometer is presented in figure 37. Two notch filters (50 Hz and 150 Hz) have been used for the elimination of the power frequency components. The tuned integration circuit (for voltage coil input) or current-to-voltage converter (for current coil input) can be selected by the investigator. Due to the high sensitivity of the sensor the smallest attainable sensitivity of the magnetometer was found to be 0.1 pT.

By applying the special design of a sensor and electronics it is possible to extend the working range towards high frequencies, to the MHz range. Cavoit [4] designed a large primary shorted coil (with small capacity and high resonance frequency) coupled to a toroidal ferrite core bearing a winding (figure 38). Prototypes of such sensors, used for radar and space probes, worked at a frequency range of 0.1–50 MHz.

The interest in the measurement of high frequency magnetic fields (up to several GHz) grew with the latest rapid development of high frequency applications, for example mobile phones and their antennae. The inductive sensor can also be used in this range of frequencies, although several additional problems can occur [81]. The dimensions of the sensor should be smaller than the wavelength of the measured field. Therefore, typically measuring instruments are equipped with several sensors. An example of a high frequency field sensor is presented in figure 39. Additional problems arise from the fact that in a high frequency electromagnetic field it is rather difficult to separate the electric and magnetic components (especially near the source of the field).

Coil sensor antennas can be used as pickup coil sensors for the detection of metal objects [82, 83]. An example of such

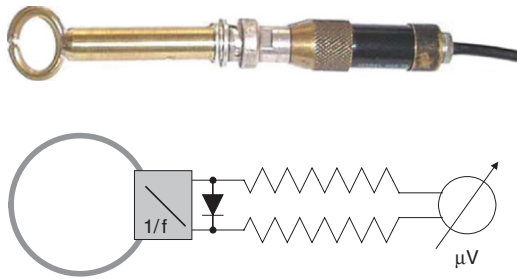


**Figure 39.** Magnetic field sensor for the frequency bandwidth of 0.6–2 GHz.



**Figure 40.** An induction search coil as a tool for the detection of metal objects (with permission of DCG Detector Center).

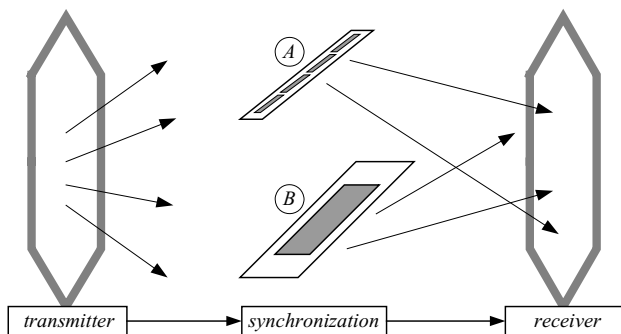


**Figure 41.** Magnetic article surveillance system: (A) magnetic harmonic system, (B) magneto-acoustic system.

a device is shown in figure 40. Practically almost all mine detectors use coil sensors [84, 85, 86]. Especially important are applications of magnetic sensors in water environment, for submarine communication and location of submarines [87, 88].

Induction coil sensors are commonly used in geophysics, for the observation of magnetic anomaly and low-frequency fields. An interesting application of such investigations is the possibility of prognosis of earthquake events, probably due to the signals generated by piezoelectric rock formation before the earthquake [89–92].

Great commercial success can be noted in the application of magnetic antennae in magnetic article surveillance systems (figure 41). Two main types of such systems are used.

In the first [93], thin strips cut from amorphous materials are magnetized by the field emitted from the transmitter antenna. Due to the nonlinearity of the magnetic properties the output signal contains harmonics of the predetermined frequency detectable by the receiver antenna.

Recently, a more efficient magneto-acoustic system was proposed by Herzer [94]. The label is prepared as a strip made from magnetostrictive amorphous material. A transmitter produces pulses of frequency of 58 kHz, 2 ms on and 20 ms off. The vibrating amorphous strip generates a signal of frequency of 58 kHz, which is detected by the receiving antenna. The system is synchronized, so the antenna is active only during the pause, and therefore the influence of background noise is decreased.

In both systems the activation or deactivation of the marker is realized by an additional strip made from a semi-hard magnetic material. After demagnetization of this initially magnetized element, the frequency generated by the label changes and it is not detected by the receiver antenna, thus deactivation is achieved.

## 9. Conclusion

The induction sensors used for magnetic field measurements (and indirectly other quantities such as for example current) have been known for many years. Today, they are still in common use for their important advantages: simplicity of operation and design, wide frequency bandwidth and large dynamics.

The performance of the induction coil sensor can be precisely calculated due to the simplicity of the transfer function  $V = f(B)$ . All factors (number of turns and cross-section area) can be accurately determined and because function  $V = f(B)$  does not include material factors (potentially influenced by external conditions such as temperature) their dependence is excellently linear without upper limit (without saturation).

Because of the absence of any magnetic elements and excitation currents, the sensor practically does not disturb the measured magnetic field (as compared for instance with fluxgate sensors).

The case of a coil sensor with ferromagnetic core is more complicated, because the permeability depends on the magnetic field value and/or temperature. Despite this, if the core is well designed, then these influences can be significantly reduced.

However, the coil sensors also exhibit some shortcomings. First, they are sensitive only to ac magnetic fields, although quasi-static magnetic fields (of frequencies down to mHz range) can be measured. One notable inconvenience is that the output signal does not depend on the magnetic field value but on the derivative of this field  $dB/dt$  or  $dH/dt$ . Therefore, the output signal is frequency dependent. Moreover, it is necessary to connect an integrating circuit to the sensor, which can introduce additional errors of signal processing.

It is rather difficult to miniaturize the induction coil sensors because their sensitivity depends on the sensor area (or the length of the core). Nevertheless, micro-coil sensors with dimensions less than 1 mm that have been prepared through the use of thin film techniques are reported.

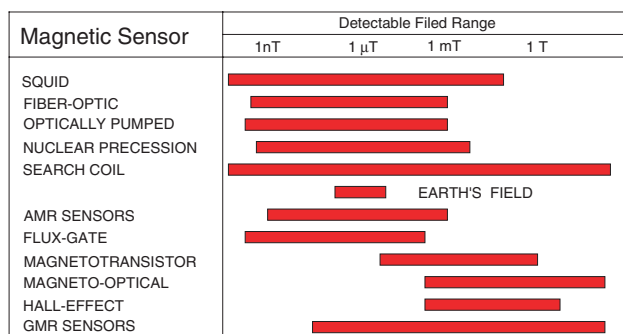


**Figure 42.** The typical field range of various magnetic field sensors.

Two methods are used for the output electronic circuit: the integrator circuit and the current-to-voltage transducer (self-integration mode). Although digital integration techniques are developed and commonly used, the analogue techniques, especially current-to-voltage transducers, are often applied due to their simplicity and good dynamics.

Certain old inventions, such as the Chattock–Rogowski coil or the needle method, are today successfully re-utilized. The importance of the coil sensor has also increased recently, because it is easy to measure stray fields generated by electrical devices (to meet electromagnetic compatibility requirements).

The induction coil sensors with ferromagnetic core prepared from modern amorphous materials exhibit sensitivity comparable to the sensitivity of SQUID sensors. But low magnetic field applications (at less than pT level) can be better served by using SQUID methods. On the other hand, it is more convenient to use the Hall sensors for large magnetic fields (above 1 mT).

Also other competitive sensors (flux-gate sensors for fields below around 100  $\mu$ T and magnetoresistive sensors for fields above around 100  $\mu$ T) are ‘winners’ in many applications—especially when miniaturization is required. For example, a spectacular ‘defeat’ was the substitution of inductive reading heads in hard drives by magnetoresistive sensors [95].

From the comparison presented in figure 42 it would be possible to conclude that the coil sensor is ‘the best’ because it covers the whole detectable field range. But in practice we should also compare other parameters, such as frequency range and dimensions. If we are not limited to the dimensions (for example in geophysical investigations) it is assumed that inductive sensors are more sensitive than fluxgates starting from the frequencies of about 0.003 Hz [3]. But if we compare the sensors of the same dimensions this border is shifted to about 10 Hz [27].

In most sensors, the practical limit of the resolution depends on the possibility of achieving the noise floor. In the comparison of various magnetic field sensors, Prance *et al* [3] estimated these noise levels as:  $\sim 50$  fT Hz $^{-1/2}$  for SQUID,  $< 100$  fT Hz $^{-1/2}$  for induction coil,  $\sim 100$  fT Hz $^{-1/2}$  for fluxgates,  $\sim 1$  pT Hz $^{-1/2}$  for optically pumped magnetometers,  $\sim 100$  pT Hz $^{-1/2}$  for magnetoresistive sensors and  $\sim 10$  nT Hz $^{-1/2}$  for Hall sensors. This comparison is presented in figure 43.

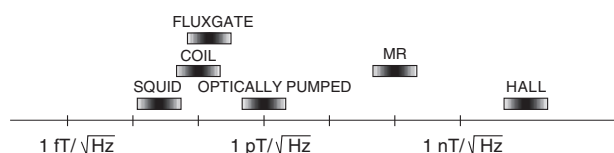


**Figure 43.** Typical resolution of various magnetic field sensors.

Examples of modern sensors and applications presented in this review demonstrate that inductive sensors still play a very important role in measuring technology.

## References

- [1] Dehmel G 1989 Magnetic field sensors: induction coil (search coil) sensors *Sensors—A Comprehensive Survey* vol 5 (New York: VCH) pp 205–54 chapter 6
- [2] Ripka P 2001 Induction sensors *Magnetic Sensors and Magnetometers* (Boston, MA: Artech House) pp 47–74 chapter 2
- [3] Prance R J, Clark T D and Prance H 2006 Room temperature induction magnetometers *Encyclopedia of Sensors* vol 10 ed C A Grimes, E C Dickey and M V Pishko (Valencia, CA: American Scientific Publishers) pp 1–12
- [4] Cavoit C 2006 Closed loop applied to magnetic measurements in the range of 0.1–50 MHz *Rev. Sci. Instrum.* **77** 064703
- [5] Zijlstra H 1967 *Experimental Methods in Magnetism* (Amsterdam: North-Holland)
- [6] Rogowski W and Steinhaus W 1912 Die Messung der magnetischen Spannung (The measurements of magnetic potential) *Arch. Elektrotechnik* **1** 141–50
- [7] Chattock A P 1887 On a magnetic potentiometer *Phil. Mag.* **24** 94–6
- [8] Murgatroyd P 1996 Progress with Rogowski coils *EMCWA Conf. (Chicago, IL)* pp 369–74
- [9] Shirkoohi G H and Kontopoulos A S 1994 Computation of magnetic field in Rogowski–Chattock potentiometer compensated magnetic tester *J. Magn. Magn. Mater.* **133** 587–90
- [10] Werner E 1957 Einrichtung zur Messung magnetischer Eigenschaften von Blechen bei Wechselstrommagnetisierung, (The device for testing of electrical steel magnetized by AC field) *Austrian patent* no. 191015
- [11] Senda K, Ishida M, Sato K, Komatsubara M and Yamaguchi T 1997 Localized magnetic properties in grain-oriented silicon steel measured by stylus probe method *Trans. IEEE Japan* **117-A** 941–50
- [12] Pfützner H and Krismanic G 2004 The needle method for induction tests – sources of error *IEEE Trans. Magn.* **40** 1610–6
- [13] Prance R J, Clark T D and Prance H 2003 Compact room-temperature induction magnetometer with superconducting quantum interference level field sensitivity *Rev. Sci. Instrum.* **74** 3735–9
- [14] Richter W 1979 Induction magnetometer for biomagnetic fields (Induktionsmagnetometer für biomagnetische Felder) *Exp. Technik Phys.* **27** 235–43
- [15] Herzog R F K and Tischler O 1953 Measurement of inhomogeneous magnetic fields *Rev. Sci. Instrum.* **24** 1000–1
- [16] Stuart W F 1972 Earth’s field magnetometry *Rep. Prog. Phys.* **35** 803–81
- [17] Campbell W H 1969 Induction loop antennas for geomagnetic field variation measurements *ESSA Technical Report* ERL123-ESL6
- [18] Estola K P and Malmivuo J 1982 Air-core induction coil magnetometer design *J. Phys. E: Sci. Instrum.* **15** 1110–3

- [19] Macintyre S A 1980 A portable low noise low frequency three-axis search coil magnetometer *IEEE Trans. Magn.* **16** 761–3
- [20] Schilstra G and van Hateren J H 1998 Using miniature sensor coils for simultaneous measurement of orientation and position of small, fast-moving animals *J. Neurosci. Methods* **83** 125–31
- [21] Gatzten H H, Andreeva E and Iswahjudi H 2002 Eddy-current microsensors based on thin-film technology *IEEE Trans. Magn.* **38** 3368–70
- [22] Sadler D J and Ahn C H 2001 On-chip eddy current sensor for proximity sensing and crack detection *Sensors Actuators A* **91** 340–5
- [23] Hirota T, Siraiwa T, Hiramoto K and Ishihara M 1993 Development of micro-coil sensor for measuring magnetic field leakage *Japan. J. Appl. Phys.* **32** 3328–9
- [24] Mukhopadhyay S C, Yamada S and Iwahara M 2002 Experimental determination of optimum coil pitch for a planar mesh-type micromagnetic sensor *IEEE Trans. Magn.* **38** 3380–82
- [25] Zhao L, van Wyk J D and Odendaal W G 2004 Planar embedded pick-up coil sensor for integrated power electronic modules *Appl. Power Electron. Conf.* **2** 945–51
- [26] Uesaka M, Hakuta K, Miya K, Aoki K and Takahashi A 1998 Eddy-current testing by flexible microloop magnetic sensor array *IEEE Trans. Magn.* **34** 2287–97
- [27] Tumanski S 1986 Analiza mozliwosci zastosowania magnetometrow indukcyjnych do pomiaru indukcji slabych pol magnetycznych (in Polish) (Analysis of induction coil performances in application for measurement of weak magnetic field) *Przeglad Elektr.* **62** 137–41
- [28] Prance R J, Clark T D and Prance H 2000 Ultra low noise induction magnetometer for variable temperature operation *Sensors Actuators* **85** 361–4
- [29] Ueda H and Watanabe T 1980 Linearity of ferromagnetic core solenoids used as magnetic sensors *J. Geomagn. Geoelectr.* **32** 285–95
- [30] Hayashi K, Oguti T, Watanabe T and Zambresky L F 1978 Absolute sensitivity of a high- $\mu$  metal core solenoid as a magnetic sensor *J. Geomagn. Geoelectr.* **30** 619–30
- [31] Ness N F 1970 Magnetometers for space research *Space Sci. Rev.* **11** 459–554
- [32] Korepanow V E 2003 The modern trends in space electromagnetic instrumentation *Adv. Space. Res.* **32** 401–6
- [33] Korepanov V and Berkman R 2001 Advanced field magnetometers comparative study *Measurement* **29** 137–46
- [34] Frandsen A M A, Holzer R E and Smith E J 1969 OGO search coil magnetometer experiments *IEEE Trans. Geosci. Electr.* **7** 61–74
- [35] Seran H C and Fergeau P 2005 An optimized low-frequency three-axis search coil magnetometer for space research *Rev. Sci. Instrum.* **76** 1–10
- [36] Internet: <http://www.meda.com>
- [37] Cavoit C 2006 Closed loop applied to magnetic measurements in the range of 0.1–50 MHz *Rev. Sci. Instrum.* **77** 064703
- [38] Yabukami S, Kikuchi K, Yamaguchi M and Arai K I 1997 Magnetic flux sensor principle of microstrip pickup coil *IEEE Trans. Magn.* **33** 4044–6
- [39] Yamaguchi M, Yabukami S and Arai K I 2000 Development of multiplayer planar flux sensing coil and its application to 1 MHz–3.5 GHz thin film permeance meter *Sensors Actuators* **81** 212–5
- [40] Ueda H and Watanabe T 1975 Several problems about sensitivity and frequency response of an induction magnetometer *Sci. Rep. Tohoku Univ., Ser. 5. Geophys.* **22** 107–27
- [41] Clerc G and Gilbert D 1964 La contre-reaction de flux appliqué aux bobines à noyau magnétique utilisée pour l'enregistrement des variations rapides du champ magnétique (The feedback of magnetic flux used for measurements of magnetic field by means of coil sensor) *Ann. Geophys.* **20** 499–502
- [42] Micheel H J 1987 Induktionsspulen mit induktiver Gegenkopplung als hochauflösende Magnetfeldsonden (The coil with inductive feedback used as magnetic field sensor) *NTZ Archiv.* **9** 97–102
- [43] Sklyar R 2006 Suppression of low-frequency interferences in the induction sensor of magnetic field *Measurement* **39** 634–42
- [44] Scholes R 1970 Application of operational amplifiers to magnetic measurements *IEEE Trans. Magn.* **6** 289–91
- [45] Pettinga J A and Siersema J 1983 A polyphase 500 kA current measuring system with Rogowski coils *IEE Proc. B* **130** 360–3
- [46] Smith R S and Annan A P 2000 Using an induction coil sensor to indirectly measure the B-field response in the bandwidth of the transient electromagnetic method *Geophysics* **65** 1489–94
- [47] D'Antona G, Carminati E, Lazzaroni M, Ottoboni R and Svelto C 2002 AC current measurements via digital processing of Rogowski coils signal *IEEE Instrum. Meas. Technol. Conf. (Anchorage, AL)* pp 693–8
- [48] D'Antona G, Lazzaroni M, Ottoboni R and Svelto C 2003 AC current-to-voltage transducer for industrial application *IEEE Instrum. Meas. Technol. Conf. (Vail)* pp 1185–90
- [49] Eriksson T, Blomgren J and Winkler D 2002 An HTS SQUID picovoltmeter used as preamplifier for Rogowski coil sensor *Physica C* **368** 130–3
- [50] Groszkowski J 1937 The vibration magnetometer *J. Sci. Instrum.* **14** 335–39
- [51] Hagedorn W and Mende H H 1976 A method for inductive measurement of magnetic flux density with high geometrical resolution *J. Phys. E: Sci. Instrum.* **9** 44–6
- [52] Hetrick R E 1989 A vibrating cantilever magnetic field sensor *Sensors Actuators* **16** 197–207
- [53] Jiles D 1998 *Magnetism and Magnetic Materials* (London: Chapman & Hall)
- [54] Karp P and Duret D 1980 Unidirectional magnetic gradiometers *J. Appl. Phys.* **51** 1267–72
- [55] Senaj V, Guillot G and Darrasse L 1998 Inductive measurement of magnetic field gradients for magnetic resonance imaging *Rev. Sci. Instrum.* **69** 2400–5
- [56] Fagaly R L 2001 Superconducting quantum interference devices *Magnetic Sensors and Magnetometers* (Boston, MA: Artech House) pp 305–47 chapter 8
- [57] Nafalski A, Moses A J, Meydan T and Abousetta M M 1989 Loss measurements on amorphous materials using a field-compensated single strip tester *IEEE Trans. Magn.* **25** 4287–91
- [58] Khnalou A, Moses A J, Meydan T and Beckley P 1995 A computerized on-line power loss testing system for the steel industry, based on the Rogowski Chattock potentiometer compensation technique *IEEE Trans. Magn.* **31** 3385–7
- [59] Stoll R L 1975 Method of measuring alternating currents without disturbing the conducting circuit *IEE Proc.* **122** 1166–7
- [60] Pellinen D G, di Capua M S, Sampayan S E, Gerbracht H and Wang M 1980 Rogowski coil for measuring fast, high-level pulsed currents *Rev. Sci. Instrum.* **51** 1535–40
- [61] Nassisi V and Luches A 1979 Rogowski coils: theory and experimental results *Rev. Sci. Instrum.* **50** 900–2
- [62] Ward D A and Exon J L T 1993 Using Rogowski coils for transient current measurements *Eng. Sci. Educ. J.* **2** 105–13
- [63] Bellm H, Küchler A, Herold J and Schwab A 1985 Rogowski-Spulen und Magnetfeldsensoren zur Messung transierter Ströme im Nanosekundenbereich, (The Rogowski coil and magnetic field sensors used for measurements of the current pulses in nanosecond range) *Arch. Elektr.* **68** 63–74
- [64] Murgatroyd P N, Chu A K Y, Richardson G K, West D, Yearley G A and Spencer A J 1991 Making Rogowski coils *Meas. Sci. Technol.* **2** 1218–9

- [65] Murgatroyd P 1992 Making and using Rogowski coil *ICWA Conf. (Cincinnati, OH)* pp 267–74
- [66] Murgatroyd P and Woodland D N 1994 Geometrical properties of Rogowski sensors *IEE Coll. on Low Frequency Power Measurement and Analysis (London)* pp 901–10
- [67] Ramboz J D 1996 Machinable Rogowski coil, design and calibration *IEEE Trans. Instrum. Meas.* **45** 511–5
- [68] Internet: <http://www.rocoil.co.uk>
- [69] Brown F W and Sweer J H 1945 The flux ball – a test coil for point measurements of inhomogeneous magnetic field *Rev. Sci. Instrum.* **16** 276–9
- [70] Pfützner H and Schönhuber P 1991 On the problem of the field detection for single sheet testers *IEEE Trans. Magn.* **27** 778–85
- [71] Nakata T, Ishihara Y, Nakaji M and Todaka T 2000 Comparison between the H-coil method and the magnetizing current method for the single sheet tester *J. Magn. Magn. Mater.* **215–6** 607–10
- [72] Nakata T, Kawase Y and Nakano M 1987 Improvement of measuring accuracy of magnetic field strength in single sheet testers by using two H-coils *IEEE Trans. Magn.* **23** 2596–8
- [73] Tumanski S 2002 A multi-coil sensor for tangential magnetic field investigations *J. Magn. Magn. Mater.* **242–5** 1153–6
- [74] Yamaguchi T, Senda K, Ishida M, Sato K, Honda A and Yamamoto T 1998 Theoretical analysis of localized magnetic flux measurement by needle probe *J. Physique IV* **8** 717–20 Pr2
- [75] Senda K, Ishida M, Sato K, Komatsubara M and Yamaguchi T 1999 Localized magnetic properties in grain-oriented electrical steel measured by needle probe method *Electr. Eng. Japan* **126** 942–9
- [76] Loisos G and Moses A J 2001 Critical evaluation and limitations of localized flux density measurements in electrical steels *IEEE Trans. Magn.* **37** 2755–7
- [77] Oledzki J and Tumanski S 2003 Pomiary indukcji magnetycznej w blachach elektrotechnicznych metoda iglowa, (in Polish) (Measurements of the flux density in electrical steels by means of the needle method) *Przegl. Elektr.* **79** 163–6
- [78] Krismanic G, Pfützner H and Baumgartinger N 2000 A hand-held sensor for analyses of local distribution of magnetic fields and losses *J. Magn. Magn. Mater.* **215–6** 720–2
- [79] ICNIRP (International Commission on Non-Ionizing Radiation Protection) and WHO (World Health Organization) 1999 *Guidelines on Limiting Exposure to Non-Ionizing Radiation*
- [80] Internet: <http://www.narda-sts.com>
- [81] Grudzinski E and Rozwalka K 2004 Szerokopasmowe pomiary pola magnetycznego w ochronie srodowiska—stan obecny i kierunki rozwoju, (in Polish) (A wideband magnetic field measurements in environment protection—state of the art and new trends) *Przegl. Elektr.* **80** 81–8
- [82] Internet: [www.detectorcenter.de](http://www.detectorcenter.de)
- [83] Internet: [www.aquascan.co.uk](http://www.aquascan.co.uk)
- [84] Riggs L S, Cash S and Bell T 2002 Progress toward an electromagnetic induction mine discrimination system *Proc. SPIE* **4742** 736–45
- [85] Black C, McMichael I and Riggs L 2005 Investigation of an EMI sensor for detection of large metallic objects in the presence of metallic clutter *Proc. SPIE* **5794** 320–7
- [86] Clem T R 1997 Advances in the magnetic detection and classification of sea mines and unexploded ordnance *Nav. Res. Rev.* **49** 29–45
- [87] Ioannidis G 1977 Identification of a ship or submarine from its magnetic signature *IEEE Trans. Aerosp. Electr. Syst.* **13** 327–9
- [88] Murray I B and McAuly A D 2004 Magnetic detection and localization using multichannel Levinson–Durbin algorithm *Proc. SPIE* **5429** 561–6
- [89] Fraser-Smith A C, Bernardi A, McGill P R, Ladd M E, Helliwell R A and Villard O G Jr 1990 Low-frequency magnetic field measurements near the epicenter of the  $M_s$  7.1 Loma Prieta earthquake *Geophys. Res. Lett.* **17** 1465–8
- [90] Fenoglio M A, Johnston M J S and Byerlee J D 1995 Magnetic and electric fields associated with changes in high pore pressure in fault zones: application to the Loma Prieta ULF emissions *J. Geophys. Res.* **100** 12951–8
- [91] Karakelian D, Klemperer S L, Fraser-Smith A C and Thompson G A 2002 Ultra-low frequency electromagnetic measurements associated with the 1998  $M_w$  5.1 San Juan Bautista earthquake and implications for mechanisms of electromagnetic earthquake precursors *Tectonophysics*. **359** 65–79
- [92] Surkov V V and Hayakawa M 2006 ULF geomagnetic perturbations due to seismic noise produced by rock fracture and crack formation treated as a stochastic process *Phys. Chem. Earth* **31** 273–80
- [93] *US Patent* 4484184 1984 Amorphous antipilferage marker
- [94] *US Patent* 58413348 1998 Amorphous magnetostrictive alloy and surveillance system employing same
- [95] Tumanski S 2000 *Thin Film Magnetoresistive Sensors* (Bristol: Institute of Physics Publishing)